Part II Applied Physics

Section 1 Atomic, Molecular and Optical Physics

Chapter 1. Quantum Optics and Photonics

Academic and Research Staff

Professor Shaoul Ezekiel, Dr. Mara G. Prentiss

Visiting Scientists and Research Affiliates

Dr. Philip R. Hemmer, John Kierstead, Dr. Elias Snitzer[1]

Graduate Students

M. Selim Shahriar, Stephen P. Smith, Farhad Zarinetchi, John Donoghue

Technical and Support Staff

Margaret McCabe

1.1 Microwave Phase Dependent Optical Absorption

Sponsor

Rome Air Development Center

A laser excited resonant Raman interaction causes atoms to be optically pumped into a non-absorbing dressed state, called the trapped state.[2] We have shown how a microwave field can modify this non-absorbing state in a phase sensitive way to produce changes in the absorption of the optical Raman excitation fields.

Figure 1 shows a three-level atomic system in the lambda configuration, where ω_1 and ω_2 are the frequencies of the laser fields which excite the Raman transition, and ω_3 is the frequency of the microwave field. Here it is assumed that states 1 and 3 are long-lived, but state 2 is short-lived with a decay rate of y_2. The Raman trapped state has the form

$$[|1> |\omega_1> - |3> |\omega_2>]/\sqrt{2},$$

where equal Rabi frequencies have been assumed, and $|\omega_1>$ and $|\omega_2>$ are single photon states. In comparison, the high and low energy dressed states of the single photon $1 \leftrightarrow 3$ microwave transition are

$$[|1> |\omega_3> - |3>]/\sqrt{2}$$

and

$$[|1> |\omega_3> + |3>]/\sqrt{2},$$

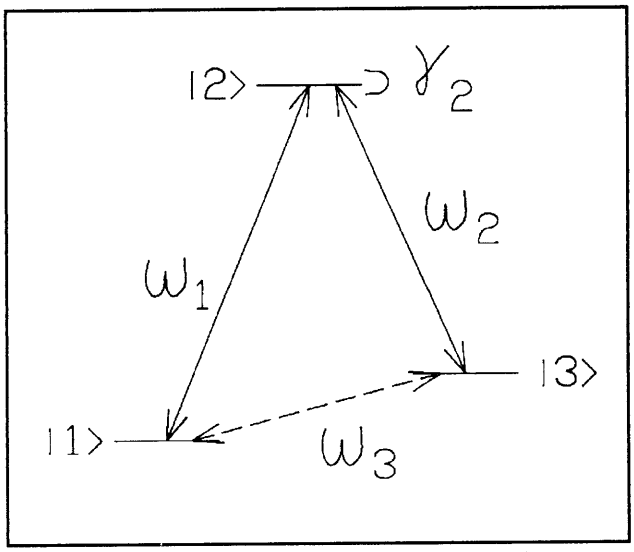

Figure 1. Three level atomic system showing resonance Raman excitation fields ω_1 and ω_2 and microwave field ω_2.

---

[1] Rutgers University, New Jersey.

[2] H.R. Gray, R.M. Whitley, and C.R. Stroud, Jr., "Coherence Trapping of Atomic Populations," *Opt. Lett.* 3:218 (1978).

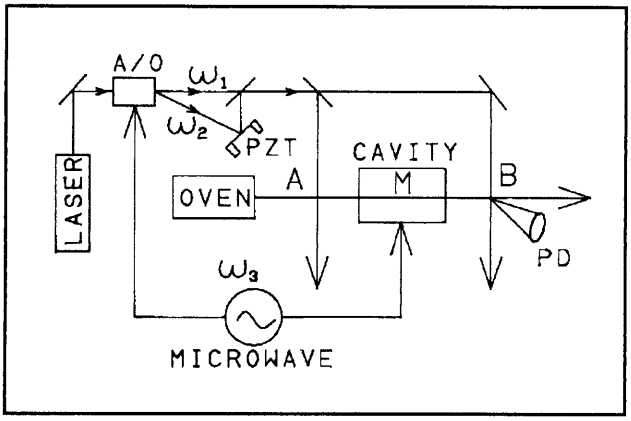

Figure 2. Schematic of experimental setup.

respectively.[3]

When the laser difference frequency $\omega_1 - \omega_2$ is exactly in (or out of) phase with the microwave frequency ω_2, the Raman trapped state translates directly into the high (or low) energy microwave dressed state. For any other value of phase difference, a linear combination of microwave dressed states results. In this case, the microwave interaction partially destroys the Raman trapped state, resulting in increased optical absorption. Thus, the optical absorption is sensitive to microwave phase.

To observe this effect, we used a three-zone sodium atomic beam apparatus as illustrated schematically in figure 2. Here the interaction in zone A optically pumps the sodium atoms into the Raman trapped state. These prepared atoms then interact with a microwave field inside the cavity (zone M) and the changes in optical absorption are monitored in zone B via fluorescence induced with a Raman probing interaction. With no microwave field, the Raman-Ramsey fringe lineshape of figure 3a is observed.[4] However, when microwave power corresponding to a π-pulse is present in zone M, the lineshape of figure 3b results. The oscillations shown by this data are produced by a rapid scanning of the relative microwave and laser difference frequency phases via the PZT (figure 2). Large changes in optical absorption are produced by changing only the relative phase of the microwave field. Figure 3c shows the corresponding theoretical lineshape which includes the effect of velocity averaging in the atomic beam. The preliminary data shows qualitatively good agreement between theory and experiment.

There would be many applications for this technique if the microwave transition could be replaced by a mm-wave or FIR transition. For example, if a mm-wave or FIR beam and a double optical beam intersect at an angle, the resulting spatial dependence of the relative phase would produce a grating-like diffraction of both beams. This double diffraction effect may have applications in beam steering and, possibly, in converting real time holographic images.

1.2 A New Approach to Microwave Excitation of Atomic Beams

A beam of alkali atoms, e.g., sodium, initially state-prepared into one of the ground state hyperfine levels, undergoes Rabi flopping when passed through a microwave cavity excited by a resonant microwave frequency.[5] Figure 4, plot I, shows how the amplitude of the oscillating B field is usually configured in the cavity. The population change is maximum when the microwave field strength corresponds to a π-pulse for the transit time. If the microwave frequency is scanned, the familiar Lorentzian lineshape (figure 5a, dashed line) is observed, its linewidth determined by transit time and power broadening. Figure 4, plot II, shows that, if the field

---

[3] Y.S. Bai, A.G. Yodh, T.W. Mossberg, "Selective Excitation of Dressed Atomic States by Use of Phase-Controlled Optical Fields," *Phys. Rev. Lett.* 55:1277 (1985).

[4] J.E. Thomas, P.R. Hemmer, S. Ezekiel, C.C. Leiby, Jr., R.H. Picard, and C.R. Willis, "Observation of Ramsey Fringes Using a Stimulated, Resonance Raman Transition in a Sodium Atomic Beam," *Phys. Rev. Lett.* 48:867 (1982).

[5] N.F. Ramsey, *Molecular Beams.* (London: Oxford University Press, 1956).

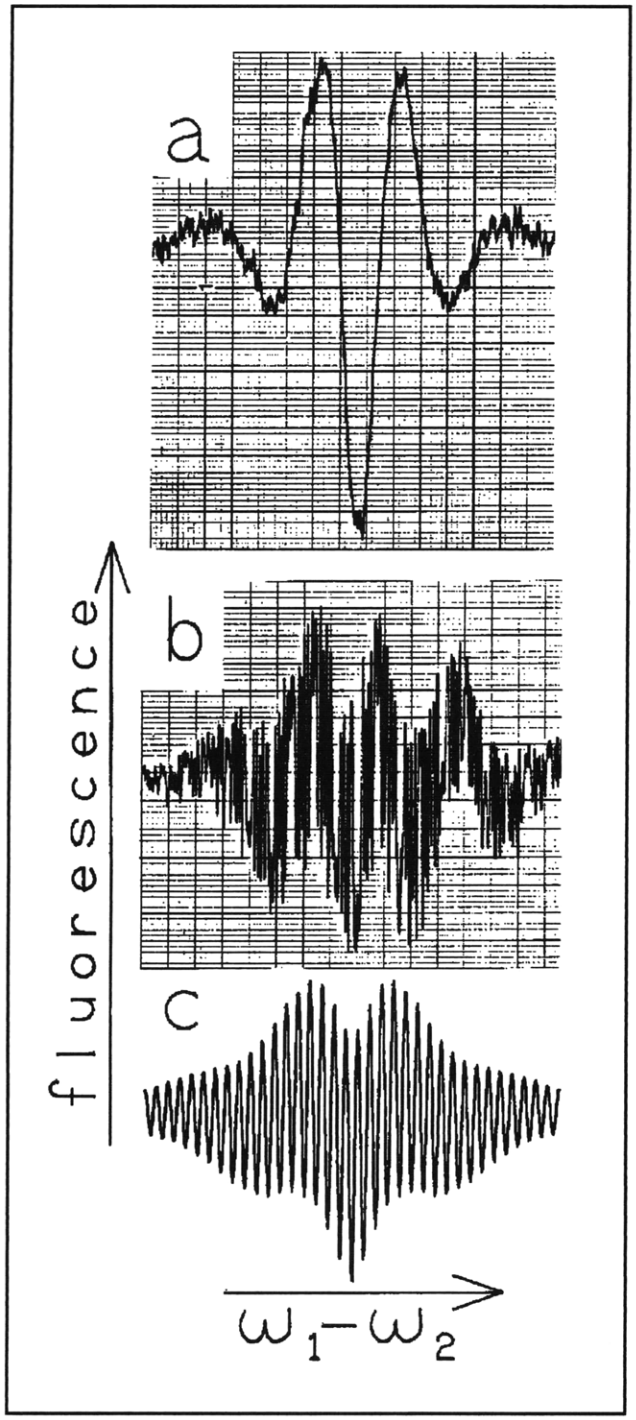

Figure 3. (a) Data showing Raman-Ramsey fringes with no microwave present. (b) Data showing modified fringes when a phase varying microwave field of π-pulse amplitude is introduced in zone M. (c) Theoretical plot corresponding to the data in (b) including the effect of velocity averaging.

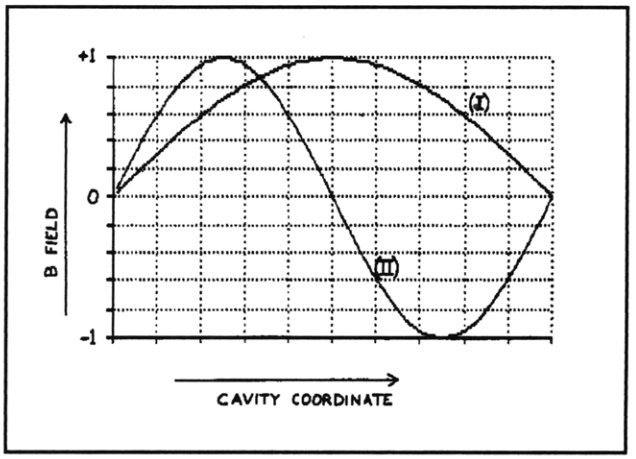

Figure 4. Cavity cross-section in a TE_{102} resonator in two different orientations. Plot I is the one usually used in microwave excitation, while Plot II is the one used here.

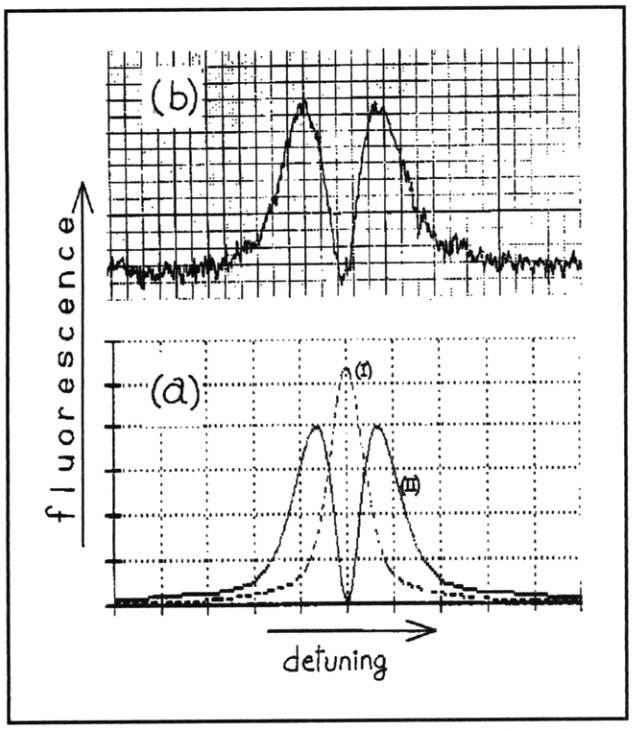

Figure 5. (a) Solid line shows the population change as a function of the microwave detuning, the dip corresponding to zero detuning. Dashed line shows the usual Lorentzian lineshape seen when there is no phase flip inside the cavity. (b) The experimental data corresponding to the solid line in (a).

profile has a node,[6] then this Lorentzian lineshape develops a dip that goes to zero on resonance. The unique property of this dip is that it goes all the way to zero even for thermal beam with a wide velocity distribution. This is different from the usual dip (inverse of figure 5a, dashed line) observed in microwave resonance, which, due to velocity averaging, always remains well above zero. In addition, unlike the usual dip, this one remains zero at all powers. We can also extend the theory behind this effect to separated field excitations, suggesting that locking microwave oscillator to this lineshape might result in reduced shot noise.

We can more easily understand the physical aspects of this effect in terms of Bloch vectors.[7] During the first half of the excitation, the vector rotates through an angle (e.g., $\pi/2$ for a $\pi/2$ pulse) in the Rabi flop plane. Next, the vector rotates by an angle π in the phase plane, continuing to rotate in the same direction in the Rabi flop plane. If the pulse strength in the two lobes is equal, the rotation in the first lobe is undone. The initial amount of rotation must be arbitrary for total cancellation to occur. Thus, cancellation would occur for any pulse strength. In addition, this implies that different atoms with different velocities would be cancelled totally. The dip, therefore, would go to zero even for a thermal beam having a wide velocity distribution and inhomogeneous transit time broadening.

When the microwave is detuned, the vector no longer rotates in the Rabi-flopping plane. This negates total cancellation and generates maximum population inversion when the amplitude of the detuning is of the order of the Rabi frequency. Thus the spectrum, as a function of detuning, appears as two peaks; the separation between them increases as the microwave power increases. Figure 5b shows a lineshape with an average microwave power corresponding to approximately a π-pulse. Figure 5a, solid line, shows the corresponding theoretical plot, with good agreement. In comparison, the dashed line in figure 5a shows the corresponding lineshape for a conventional configuration.

By changing the level with an observable population, the peak of figure 5a, dashed line, can be converted into a dip. Figure 6a shows a set of these dips (corresponding to cavity cross-section I) as the microwave Rabi frequency varies. The dip moves up and down as microwave power changes, but never moves close to zero. In contrast, figure 6b shows the dips (corresponding to cavity cross-section II) as the microwave Rabi frequency varies by the same amounts as in figure 6a. The dip is always at zero, independent of changes in microwave power. Figure 6c also shows this, illustrating that the signal at the bottom of the dip varies as a function of Rabi frequency for these two sets of lineshapes.

---

[6] J.A. Kong, *Electromagnetic Wave Theory.* (New York: John Wiley, 1988).

[7] M. Sargent III, M.O. Scully, and W.E. Lamb, Jr., *Laser Physics.* (Reading, Massachusetts: Addison-Wesley, 1979).

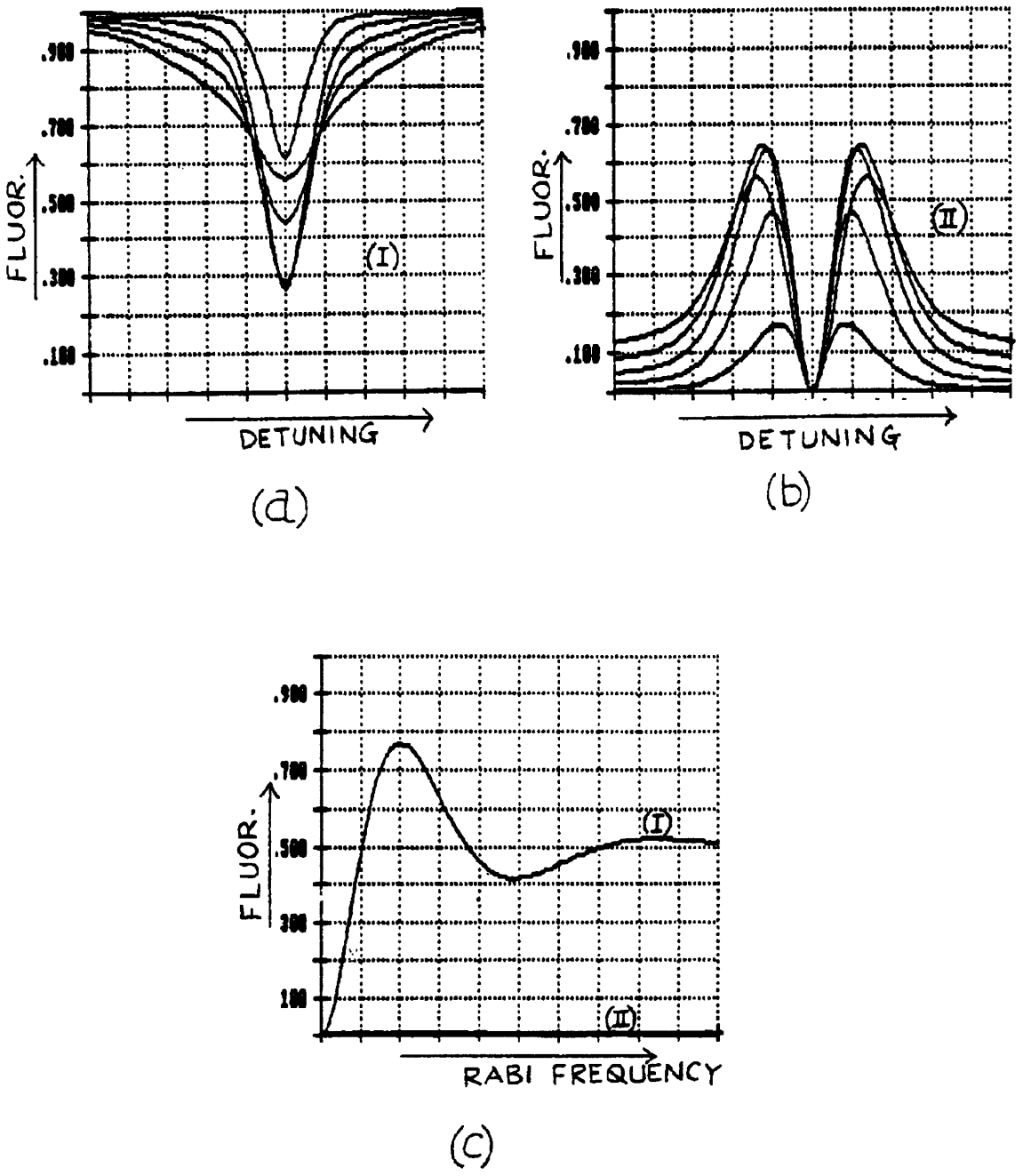

Figure 6. (a) Conventional dips for cross-section I, as the Rabi frequency is varied. (b) Corresponding set for new dips seen in cross-section II. (c) How the dips in sets I and II move as the Rabi frequency is varied continuously.

1.3 Stimulated Brillouin Fiberoptic Gyroscope

Sponsor

Charles S. Draper Laboratory

Fiberoptic inertial rotation sensors (or gyroscopes) have been based on the Sagnac effect in either a multiturn interferometer[8] or a resonator.[9] Both of these approaches constitute the fiberoptic implementation of previously demonstrated Sagnac interferometer[10] gyroscopes and resonator[11] gyroscopes that employ bulk-optic components. However, we have recently begun to study a fiberoptic analog of the ring laser gyroscope,[12] which was a bulk-optic device. In the following figures, we are presenting preliminary data on a fiberoptic ring laser gyroscope with stimulated Brillouin[13] scattering as the laser gain medium. To our knowledge, this is the first demonstration of a solid state ring laser gyroscope or RLG.

Figure 7 is a simplified diagram of a stimulated Brillouin fiberoptic gyroscope. A single frequency laser, He-Ne at 1.15 μm, is coupled into the opposite direction from a non-polarization maintaining fiberoptic ring resonator (length $\approx$ 25m; finesse $\approx$ 250; coil diameter $\approx$ 7.5cm) and acts as the pump for the stimulated Brillouin laser. The frequency of the Brillouin laser[14] is downshifted from that of the pump by the acoustic frequency in the fiber (15 GHz at 1.15 μm). The direction of the Brillouin laser is opposite from the pump's because it experiences the highest Brillouin gain. The clockwise pump in the resonator is denoted by P^- and the counterclockwise pump by P^+. The corresponding stimulated Brillouin lasers that are created by the pumps are denoted by B^- and B^+.

To maintain the highest pump intensity in the resonator, the pump laser must be held at a cavity resonance by using a feedback loop. The threshold pump intensity for Brillouin lasing depends on the length and finesse of the resonator, as well as on the wavelength of the pump. In our case, we have achieved threshold intensities as low as 60 μW at the input of the resonator.

The counterpropagating Brillouin lasers, B^+ and B^-, coupled out of the resonator using fiber coupler C_1, are brought together onto a detector via coupler C_2. In the presence of inertial rotation, a beat note is generated between B^+ and B^-, proportional to the applied rotation component normal to the plane of the resonator, which is similar to the conventional RLG.

Figure 8a shows the Brillouin beat frequency (converted to an analog signal) as a function of a sinusoidal rotation (figure 8b) applied to the table supporting the gyro. The peak beat

---

8 V. Vali and L.W. Shorthill, "Fiber Ring Interferometer," Appl. Opt. 15, 1099 (1976).

9 R.E. Meyer, S. Ezekiel, D.W. Stowe and V.J. Tekippe, "Passive Fiber Optic Ring Resonator for Rotation Sensing," *Opt. Lett.* 8:644 (1983).

10 W.R. Carrington, R. Fredricks, and Lear Siegler, Inc., *Development of an Optical Sensor: Final Report to the U.S. Office of Naval Research on Contract N00014-73-C-0377,* November 1973.

11 S. Ezekiel and S.R. Balsamo, "Passive Ring Resonator Laser Gyroscope," *Appl. Phys. Lett.* 30:478 (1977).

12 A.H. Rosenthal, "Regenerative Circulatory Multiple-Beam Interferometry for the Study of Light-Propagation Effects," *J. Opt. Soc. Am.* 52:1143 (1962); W.M. Macek and D.T.M. Davis, Jr., "Rotation Rate Sensing with Traveling Wave Ring Laser," *Appl. Phys. Lett.* 2:67 (1963).

13 P.J. Thomas, H.M. van Driel, and G.I.A. Stegeman, "Possibility of Using an Optical Fiber Brillouin Ring Laser for Inertial Sensing," *Appl. Opt.* 19:1906 (1980).

14 K.O. Hill, B.S. Kawasaki, and D.C. Johnson, "Cw Brillouin Laser," *Appl. Phys. Lett.* 28:608 (1976); D.R. Ponikvar and S. Ezekiel, "Stabilized Single-Frequency Stimulated Brillouin Fiber Ring Laser," *Opt. Lett.* 6:398 (1981); L.F. Stokes, M. Chodorow, and H.J. Shaw, "All Fiber Stimulated Brillouin Ring Laser with Submilliwatt Pump Threshold," *Opt. Lett.* 7:509 (1982); P. Bayvel and I.P. Giles, "Evaluation of Performance Parameters of Single Mode All Fiber Brillouin Ring Lasers," *Opt. Lett.* 14:581 (1989).

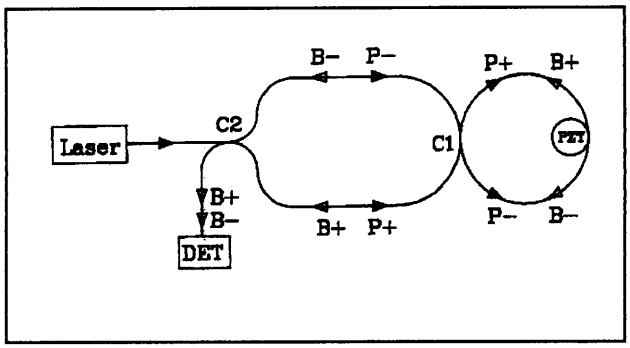

Figure 7.

frequency is about 3 kHz which is close to the 3.2 kHz value we calculated using the maximum applied rate of 3.8 deg/sec and the scale factor for the gyro. Figure 8a shows that a zero beat frequency appears whenever the rotation rate is low. This dead zone is the familiar "lock-in" phenomenon in RLGs that is caused by backscattering. The lock-in range is about 1 kHz or 1 deg/sec. Figure 7 shows that the beat frequency does not change sign with the rotation because the setup cannot detect the beat frequency phase.

In the bulk-optic RLG, use of mechanical dither overcomes the lock-in effect. In the case of the Brillouin RLG or B-RLG, we can also use mechanical dither to overcome lock-in. Other techniques, similar to those based on multiple frequency operation, can be implemented in the B-RLG, but not in the RLG.

Because the B-RLG does not require a measurement system for detecting the Sagnac effect, it has a major advantage over interferometers, which need to measure the Sagnac phase shift, and resonators that must measure frequency shift. In the B-RLG, similar to the RLG, the output is a beat frequency directly proportional to rotation rate.

We must study the preliminary data to resolve a number of issues that influence ultimate performance. At present, the B-RLG, which is basically simpler to implement and does not require highly specialized components, is a promising alternative to passive fiber interferometer and fiber resonator gyros.

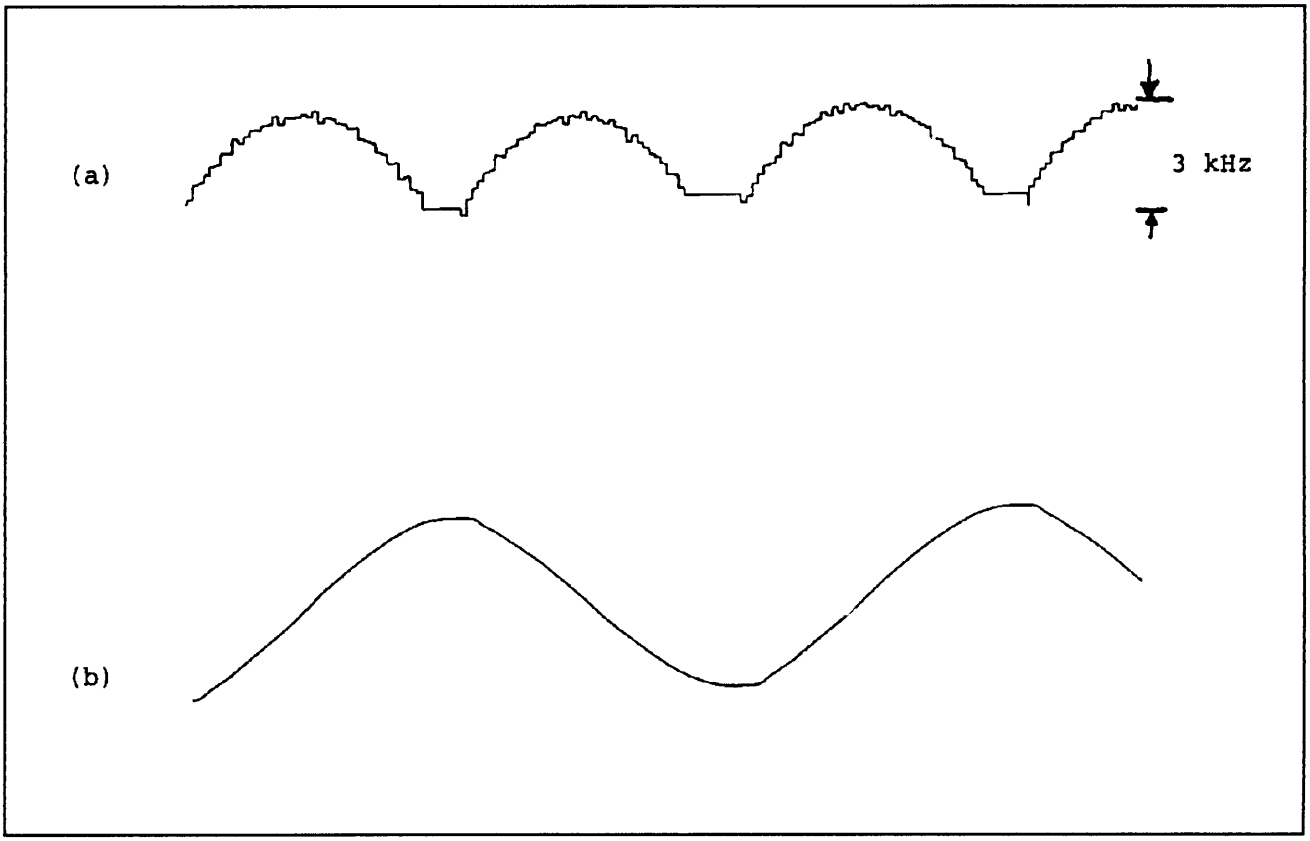

Figure 8.

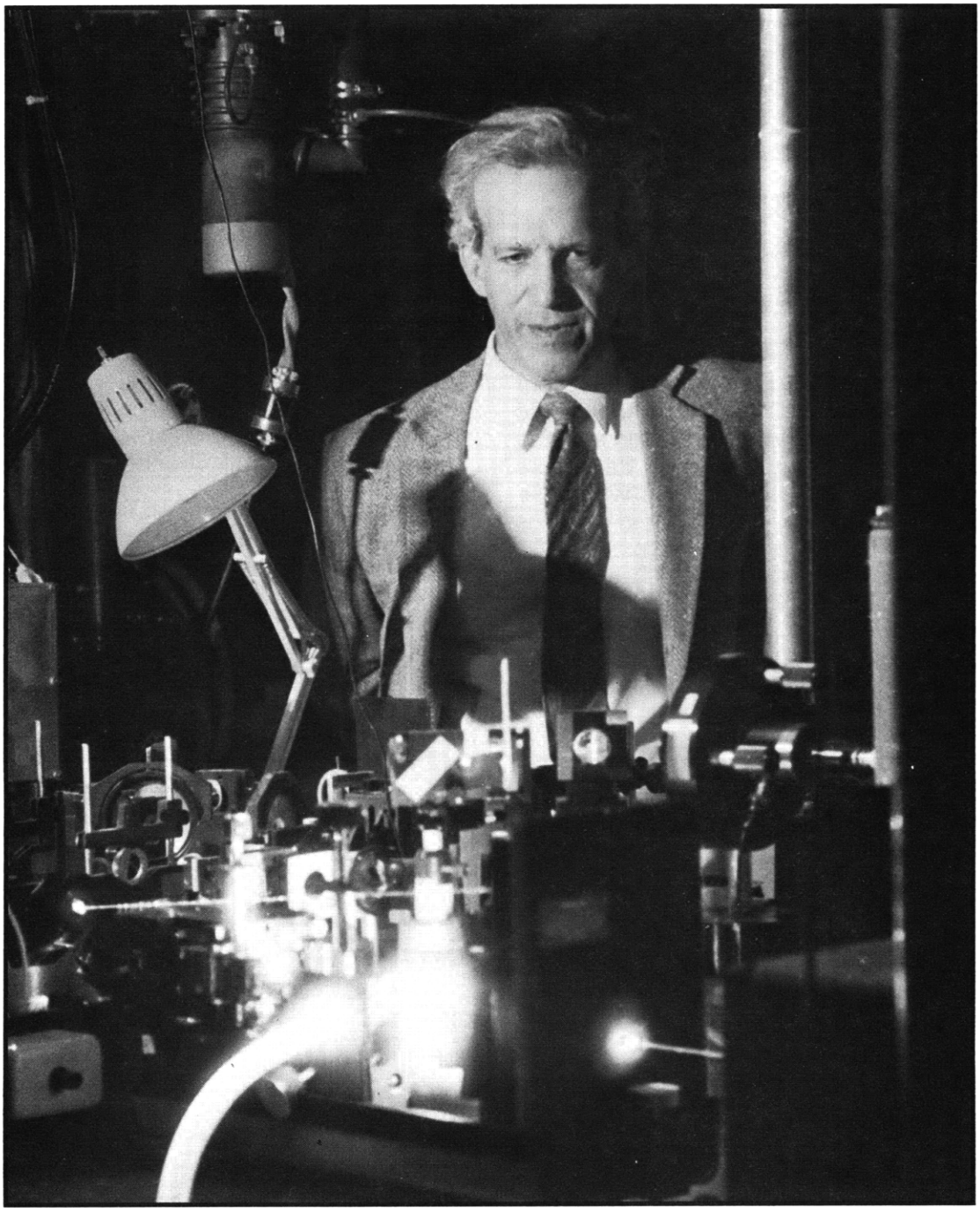

Professor Daniel Kleppner, Associate Director, Research Laboratory of Electronics